DENOISING OF SINGLE-LOOK SAR IMAGES BASED ON VARIANCE STABILIZATION AND NONLOCAL FILTERS

Markku Mäkitalo [1], Alessandro Foi [1], Dmitriy Fevralev [2], Vladimir Lukin [2]

[1] Department of Signal Processing, Tampere University of Technology,
P.O. Box FIN-553, 33101, Tampere, Finland e-mail: firstname.lastname@tut.fi

[2] National Aerospace University, Department of Transmitters, Receivers and Signal Processing,
17 Chkalova St., 61070, Kharkov, Ukraine e-mail: lukin@xai.kharkov.ua

Abstract – **Synthetic-aperture radar (SAR) imaging has become an efficient tool for obtaining and retrieving useful information about surfaces of Earth and other planets. However, the formed images suffer from speckle noise, especially if single-look observation mode is used. Then, filtering is often applied to improve image quality and provide better estimation of radar cross-section and other parameters of sensed scenes. Recently, a novel class of image filters has proved to be very successful in the removal of additive white Gaussian noise from natural images; these filters are based on *nonlocal* image modeling, i.e. they exploit the mutual self-similarity of image patches at different locations in the image. These filters have been shown in several benchmarks to significantly outperform all previous techniques. In this paper, we evaluate the performance of nonlocal filters applied to the denoising of single-look SAR images corrupted by speckle with a Rayleigh distribution, taking advantage of exact forward and inverse variance-stabilizing transformations. Numerical simulations demonstrate the success of this approach against several known despeckling methods.**

I. INTRODUCTION

Airborne and spaceborne synthetic-aperture radar (SAR) imaging is widely used in various remote sensing (RS) applications, both separately and in combination with optical sensors [1, 2]. In the former case, polarimetric, interferometric and/or multi-frequency SAR systems are often used [1, 3]. Known and widely exploited advantages of SAR imaging are its ability to provide RS data during both day and night, in bad weather conditions and with a high resolution (if single-look mode is applied) that is comparable to those of modern optical sensors. However, due to coherent processing of received (backscattered) signals, SAR images are characterized by the presence of high-intensity speckle, which is a specific kind of multiplicative noise [1, 3–8]. Speckle masks and deteriorates useful information in images, which hinders the accuracy in estimating radar cross-section and other parameters of sensed terrains.

One way to attenuate noise in SAR data is to use a multi-look imaging mode [1]. This, however, leads to a radical drop in spatial resolution, which is undesirable. Thus, a more common approach to enhance the SAR image quality is to apply filtering. Although the first (and rather efficient) filters for SAR data despeckling were already proposed about 30 years ago [5, 9, 10], efforts to improve the performance of SAR image filters still continue [8, 11, 12]. The main difficulties in designing filters for processing single-look SAR images are the multiplicative nature of the noise and the fact that its probability density function (PDF) is asymmetric with respect to its mean. From the latter arises the problem of how to preserve the mean level in homogeneous image regions [8] after filtering.

In general, a real-valued single-look SAR image can be represented in three different forms that can be quite easily recalculated to each other: the so-called intensity image, the amplitude form, and the log-intensity form [1]. For visualization purposes, the second form of SAR image representation is used most often. Thus, in what follows, we deal with the corresponding model of speckle, which can be described by a Rayleigh PDF.

The earliest SAR image despeckling methods [5, 9, 10] mainly dealt with filtering in spatial domain. Later, when orthogonal transform denoising became popular, filtering has been carried out in wavelet, discrete cosine transform (DCT) or other transform domains [6, 7, 11]. For this group of methods, denoising itself is usually carried out as an intermediate stage within a three-stage processing procedure where a direct homomorphic (variance stabilizing) transformation is applied first and the corresponding inverse homomorphic transformation is applied at the last (third) stage. In the case of speckle noise, the main goal for applying a direct homomorphic transformation is to convert multiplicative (thus heteroskedastic) noise into homoskedastic noise that can be treated as some additive white noise. Hence, these transformation are typically of logarithmic type. A main motivation for using this three-stage procedure is that there are considerably more filtering techniques designed to cope with additive noise than those intended to suppress multiplicative noise. We note that many transform-based methods can also be applied without employing

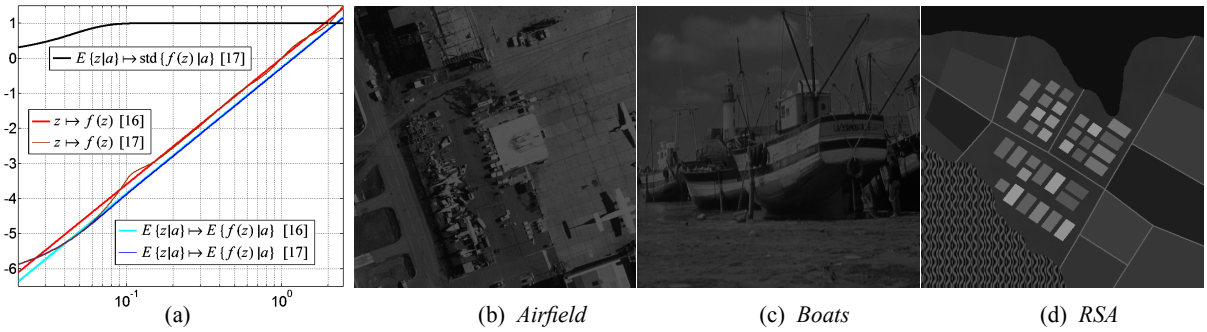

(a) (b) *Airfield* (c) *Boats* (d) *RSA*

Figure 1: (a) Plots of the exact logarithmic [16] and the approximate bounded-derivative [17] variance stabilizers f with their respective mappings $E\{z|a\} \mapsto E\{f(z)|a\}$ and $E\{z|a\} \mapsto \mathrm{std}\{f(z)|a\}$. (b-d) The three test images used for the experiments.

homomorphic transformations, leveraging instead various forms of locally adaptive thresholds (e.g., as in the DCT-based algorithm [11]).

Recently, a novel class of image filters has proved to be very successful in the removal of i.i.d. additive white Gaussian noise (AWGN) from natural images; these filters are based on *nonlocal* image modeling, i.e. they exploit the mutual self-similarity of image patches at different locations in the image. Among these novel nonlocal methods are BM3D [13] and SAFIR [14], which are among the best existing methods for removal of AWGN. It was shown in [15] that these filters can achieve state-of-the-art performance also in the removal of signal-dependent Poisson noise, when applied as an intermediate stage between variance stabilization by the Anscombe transformation and a suitable optimal inverse transformation. The goal of this paper is to evaluate the performance of nonlocal methods in conjunction with variance-stabilizing transformations, applied to speckle removal in single-look SAR images.

II. Rayleigh noise model and its variance-stabilizing transformation

Let $z \geq 0$ be a (noisy) pixel value obtained through a SAR imaging device. Then, z adheres to a Rayleigh PDF

$$p(z,a) = za^{-2}e^{-z^2/2a^2}, \quad a > 0, \tag{1}$$

where the expected value and variance of the random Rayleigh variable z are, respectively,

$$y = E\{z|a\} = a\sqrt{\pi/2}, \qquad \mathrm{var}\{z|a\} = (4-\pi)\,a^2/2. \tag{2}$$

Note that the PDF (1) becomes a Dirac delta for $a = 0$. The goal of denoising is to estimate the underlying true value y of the signal as accurately as possible. By defining the zero-mean Rayleigh noise as $n = z - E\{z|a\}$, we see that the noise variance is signal-dependent, with $\mathrm{var}\{n|y\} = \mathrm{var}\{z|y\} = \mathrm{var}\{z|a\} = (4-\pi)\,y^2/\pi$. To remove the dependence of the variance on the signal, we can apply a variance-stabilizing transformation to the obtained image data z. A suitably chosen transformation renders the noise variance constant throughout the entire image, thus enabling the use of denoising strategies designed for additive homoskedastic noise. For the Rayleigh distribution, the logarithmic transformation

$$f(z) = 2\sqrt{6}\pi^{-1}\ln(z) \tag{3}$$

stabilizes the noise variance perfectly [16], with $\mathrm{var}\{f(z)|a\} = 1$ for all $a > 0$. However, the direct application of the logarithmic transformation (3) is problematic because of the unboundedness of this function. Thus, in the following experiments, instead of (3) we use an optimized approximate stabilizer f with bounded derivative $|\partial f(z)/\partial z| \leq \delta$ for all $z \geq 0$, $\delta = 30$, obtained through the numerical procedure [17]. The plots of these stabilizers are shown in Figure 1(a).

By denoising the stabilized and transformed data, we are estimating the values of $E\{f(z)|a\}$. However, because the stabilizing transformations are necessarily nonlinear, we have $f^{-1}(E\{f(z)|a\}) \neq E\{z|a\}$, which shows that if after denoising we were to compute the final estimate of $E\{z|a\}$ by the direct algebraic inverse of f, the result would generally be biased. Thus, we utilize the exact unbiased inverse $\mathcal{I}$ that directly maps the denoised data (which, assuming the denoising is successful, equals $E\{f(z)|a\}$) to the desired values $y = E\{z|a\}$ [15]:

$$\mathcal{I} : E\{f(z)|a\} \longmapsto E\{z|a\}. \tag{4}$$

	BM3D	SAFIR	NLmeans	Lee 5×5	Lee 7×7	DCT β=2.6	DCT β=2.8	DCT β=3.0	DCT β=3.2
Airfield [0, 85]	43.58	**43.22**	67.86	142.24	144.60	50.00	45.71	44.33	44.55
Boats [0, 85]	**23.83**	23.88	46.59	103.42	102.62	29.29	25.82	24.48	24.29
RSA [10, 153]	66.98	**42.27**	105.64	205.32	222.12	89.37	84.83	84.69	87.31

Table 1: MSE results for BM3D [13], SAFIR [14], NLmeans [18], modified Lee filter [9], and DCT-based filter [11]. The former three are methods designed for AWGN, applied as intermediate steps between forward variance-stabilizing transformation and exact unbiased inverse, whereas the latter two are specifically designed for Rayleigh observations. Intensity ranges of the three test images are indicated in square brackets. All values in the table are computed with respect to a [0, 255] range.

Original Noisy BM3D SAFIR NLmeans DCT (best β)

Figure 2: Enlarged fragments of the original, noisy, and filtered images by BM3D [13], SAFIR [14], NLmeans [18], and DCT-based filter [11] (with threshold factor β minimizing the MSE).

To construct this exact unbiased inverse, it suffices to compute the values of $E\{f(z)|a\} = \int_{-\infty}^{+\infty} f(z)p(z|a)\,dz$: while in the case of (3) they equal $\sqrt{6}\pi^{-1}\left(\ln\left(2a^2\right) - c\right)$, where $c{\approx}0.5772$ is the Euler-Mascheroni constant [16], for our bounded-derivative stabilizer we resort to numerical integration of the probability integral. The plots of the mapping $E\{z|a\} \mapsto E\{f(z)|a\}$ for these two stabilizers are drawn in Figure 1(a); the corresponding exact unbiased inverses (4) can be visualized by transposing these plots.

III. Experiments

In our experiments, we consider three nonlocal denoising algorithms designed for AWGN removal, applied as intermediate stage between forward variance-stabilizing transformation and exact unbiased inverse: BM3D [13], SAFIR [14], and NLmeans [18]. For comparison with known methods for despeckling, we consider the refined local-statistic Lee filter [9] (with block sizes 5×5 and 7×7), often used in practice as well as referred to in research articles for comparisons, and the DCT-based filter [11] (with threshold factor β=2.6, 2.8, 3.0, 3.2), that has demonstrated rather good performance and is quite simple. As criterion we use the mean square error (MSE) computed as average over 5 independent noise realizations for three 512×512 images: *Airfield*, *Boats*, and the synthetic *RSA*. The images are shown in Figure 1(b-d); the intensities of the first two images have been divided by 3, in order to produce darker observations closer to actual RS images and with the noise distribution being with high probability within the imaging range. The MSE results are given in Table 1, while Figure 2 shows enlarged fragments of the original, noisy, and filtered images.

IV. Conclusions

The experiments show that BM3D and SAFIR, provided variance-stabilization, outperform the other methods for speckle-removal. In particular, the latter demonstrates a particularly good performance in dealing with images characterized by large piecewise-flat regions such as *Airfield* and *RSA*, while the former delivers better preservation of details for more varied images like *Boats*. Although NLmeans has difficulties in dealing with such strong noise, it does provide rather sharp estimates of the main structures. We note that the performance gap between NLmeans and BM3D or SAFIR is comparable to that existing in the AWGN case. The DCT-based filter is, in spite of its simplicity, quite competitive in terms of MSE. However, as can be seen particularly in the *RSA* image, it introduces visible artifacts due to the transform and, being a purely local method, is not able to reconstruct larger structures and patterns as accurately as the nonlocal filters do. The refined Lee filter performs much worse than all other methods considered here; we refer the reader to [11] and references therein for further comparisons with such classical methods.

Overall, the results are consistent with those obtained for Poisson noise reported in [15], where BM3D and SAFIR were shown to outperform all other techniques. It substantiates that state-of-the-art methods for AWGN noise removal can achieve state-of-the-art performance also in the removal of difficult non-Gaussian degradations, provided the design of suitable forward and inverse homomorphic transformations. Different constraints on the variance stabilizer for Rayleigh data will be subject of future research.

Acknowledgments

This work was supported by the Academy of Finland (projects no. 213462, Finnish Programme for Centres of Excellence in Research 2006-2011, no. 118312, Finland Distinguished Professor Programme 2007-2010, and no. 129118, Postdoctoral Researchers Project 2009-2011) and by Tampere Doctoral Programme in Information Science and Engineering (TISE).

References

[1] C. Oliver, S. Quegan, "Understanding synthetic aperture radar images", *SciTech Publishing*, 2004.

[2] O. Gungor and J. Shan, "An optimal fusion approach for optical and SAR images", *Proc. ISPRS Commission VII Mid-term Symp. "Remote Sensing: From Pixels to Processes"*, vol. 18, pp. 111-116, Enschede, Netherlands, May 2006.

[3] L. Ferro-Famil, E. Pottier, and J.S. Lee, "Unsupervised classification of natural scenes from polarimetric interferometric SAR data", *Frontiers of Remote Sensing Information Process.*, pp. 105-137, (C.H. Chen ed.), World Scientific, 2003.

[4] R. Touzi, "A review of speckle filtering in the context of estimation theory", *IEEE Trans. Geosci. Remote Sensing*, vol. 40, no. 11, pp. 2392-2404, 2002.

[5] J.S. Lee, "Speckle analysis and smoothing of synthetic aperture radar images", *Comput. Graphics Image Process.*, vol. 17, no. 1, pp. 24-32, 1981.

[6] J. Sveinsson, J. Benediktsson, "Combined wavelet and curvelet denoising of SAR images using TV segmentation", *Proc. Geosci. Remote Sensing Symposium (GARSS2007)*, pp. 503-506, Barcelona, Spain, 2007.

[7] S. Solbo and T. Eltoft, "Homomorphic wavelet-based statistical despeckling of SAR images", *IEEE Trans. Geoscience and Remote Sensing*, vol. GRS-42, no. 4, pp. 711-721, 2004.

[8] J.S. Lee and J.H. Wen, T.L. Ainsworth, et al., "Improved sigma filter for speckle filtering of SAR imagery", *IEEE Trans. Geosci. Remote Sensing*, vol. 47, no. 1, pp. 202-213, 2009.

[9] J.S. Lee, "Refined filtering of image noise using local statistics", *Comput. Graphics Image Process.*, vol. 15, no. 4, pp. 380-389, 1981.

[10] V.S. Frost and K.S. Shanmugan, "The information content of synthetic aperture radar images", *IEEE Trans. Aerospace Electronic Sys.*, vol. 19, no 5, pp. 768-774, 1983.

[11] R. Öktem, K. Egiazarian, V. Lukin, N. Ponomarenko, and O. Tsymbal, "Locally adaptive DCT filtering for signal-dependent noise removal", *EURASIP J. Advances in Signal Process.*, article ID 42472, 10 p., 2007.

[12] Z. Chen, J. Zhu, C. Li, and Y. Zhou, "A novel speckle filter for SAR images based on information-theoretic heterogeneity measurements", *Chinese J. Aeronautics (Elsevier Science Direct)*, vol. 22, pp. 528-534, 2009.

[13] K. Dabov, A. Foi, V. Katkovnik, and K. Egiazarian, "Image denoising by sparse 3D transform-domain collaborative filtering", *IEEE Trans. Image Process.*, vol. 16, no. 8, pp. 2080-2095, Aug. 2007. Software available online at http://www.cs.tut.fi/~foi/GCF-BM3D

[14] J. Boulanger, J.B. Sibarita, C. Kervrann, and P. Bouthemy, "Non-parametric regression for patch-based fluorescence microscopy image sequence denoising", *Proc. IEEE Int. Symp. Biomedical Imaging (ISBI'08)*, pp. 748-751, May 2008.

[15] M. Mäkitalo and A. Foi, "Optimal inversion of the Anscombe transformation in low-count Poisson image denoising", to appear in *IEEE Trans. Image Process.* Preprint and software available online at http://www.cs.tut.fi/~foi/invansc

[16] P.R. Prucnal and E.L. Goldstein, "Exact variance-stabilizing transformations for image-signal-dependent Rayleigh and other Weibull noise sources", *Applied Optics*, vol. 26, no. 6, March 1987.

[17] A. Foi, "Optimization of variance-stabilizing transformations", preprint available at http://www.cs.tut.fi/~foi/optvst

[18] A. Buades, B. Coll, and J. M. Morel, "A review of image denoising algorithms, with a new one," *SIAM Multiscale Modeling and Simulation*, vol. 4, no. 2, pp. 490-530, 2005. Software available online at http://www.mathworks.com/matlabcentral/fileexchange/13176